Reverse-Annealed Sequential Monte Carlo for Efficient Bayesian Optimal Experiment Design

Jake Callahan[*]
Program in Applied Mathematics
The University of Arizona

Andrew Chin[*]
Department of Biostatistics
Johns Hopkins University

Jason Pacheco
Department of Computer Science
The University of Arizona

Tommie Catanach
Computational Data Science
Sandia National Laboratories

Abstract

Expected information gain (EIG) is a crucial quantity in Bayesian optimal experimental design (BOED), quantifying how useful an experiment is by the amount we expect the posterior to differ from the prior. However, evaluating the EIG can be computationally expensive since it generally requires estimating the posterior normalizing constant. In this work, we leverage two idiosyncrasies of BOED to improve efficiency of EIG estimation via sequential Monte Carlo (SMC). First, in BOED we simulate the data and thus know the true underlying parameters. Second, we ultimately care about the EIG, not the individual normalizing constants. Often we observe that the Monte Carlo variance of standard SMC estimators for the normalizing constant of a single dataset are significantly lower than the variance of the normalizing constants across datasets; the latter thus contributes the majority of the variance for EIG estimates. This suggests the potential to slightly increase variance while drastically decreasing computation time by reducing the SMC population size, which leads us to an EIG-specific SMC estimator that starts with only a single sample from the posterior and tempers *backwards* towards the prior. Using this single-sample estimator, which we call reverse-annealed SMC (RA-SMC), we show that it is possible to estimate EIG with orders of magnitude fewer likelihood evaluations in three models: a four-dimensional spring-mass, a six-dimensional Johnson-Cook model and a four-dimensional source-finding problem.

1 Introduction

Optimal experimental design (OED) is a powerful method for selecting design parameters for experiments that update model uncertainty using observational data. By quantifying the utility U of a design d, one can maximize the utility over all the designs as: $d^* = \arg\max_d U(d)$. In Bayesian optimal experimental design (BOED) we are interested in the information gain (IG) from an experiment for an unknown parameter θ given the dataset y (Lindley, 1956). This is quantified by the Kullback-Leibler (KL) divergence from the prior to the posterior (Rainforth et al., 2024):

$$\mathrm{IG}(y \mid d) = D_{KL}(p(\theta \mid y, d) \parallel p(\theta)) = \int_\theta p(\theta \mid y, d) \log \frac{p(\theta \mid y, d)}{p(\theta)} \, \mathrm{d}\theta. \tag{1}$$

[*] Denotes equal contribution. These authors are listed in alphabetical order.

39th Conference on Neural Information Processing Systems (NeurIPS 2025).

As we do not have access to y before an experiment is run, our utility function is the expected information gain (EIG):

$$\mathrm{EIG}(d) = \mathbb{E}_{y|d}[D_{KL}(p(\theta \mid y, d) \parallel p(\theta))] = \int_y \int_\theta p(\theta, y \mid d) \log \frac{p(y \mid \theta, d)}{p(y \mid d)} \, \mathrm{d}\theta \, \mathrm{d}y \tag{2}$$

This expectation has no analytical solution outside of the most basic examples, and thus one typically resorts to Monte Carlo integration. This proceeds by drawing a dataset, estimating the IG, and repeating this many times to obtain an EIG. However, the IG itself is also generally intractable due to the presence of the posterior normalizing constant $p(y \mid d)$, also known as the model evidence or marginal likelihood. Thus, considerable effort is often placed on estimating $p(y \mid d)$ or its logarithm (Ryan, 2003), and not all methods are guaranteed to give accurate results. In low dimensions, the simple nested Monte Carlo (NMC) is a common choice (Rainforth et al., 2018; Zheng et al., 2018).

Higher dimensions or more informative data require more stable, but expensive, Monte Carlo estimators. Principal among these is a class of estimators based on sequential Monte Carlo (SMC) (Del Moral et al., 2006; Chopin et al., 2020). SMC starts with many samples from a known distribution and evolves those samples through a sequence of intermediate distributions toward the distribution of interest. Likelihood values computed during this evolutionary process can then be used to compute the model evidence (Xie et al., 2011). Often, hundreds of millions of costly likelihood evaluations are required to compute the EIG for a single design, making SMC infeasible for many models.

Our work adapts and extends the bidirectional Monte Carlo approach introduced by Grosse et al. (2015) for the specific context of BOED by leveraging two unique aspects of the problem. First, we observe that in BOED we require $\mathbb{E}[\log p(y)]$, and the variance in $\log p(y)$ across different y often dominates the variance in estimating $\log p(y)$ for a single y when using SMC. We find that we can significantly reduce the number of particles to achieve similar Monte Carlo error but with far less computational cost. The second observation is that generating y requires drawing $\theta \sim p(\theta)$ and then $y \sim p(y \mid \theta)$, resulting in the joint sample $(\theta, y) \sim p(\theta, y)$. Instead of discarding θ, we can treat this joint sample as if we drew $y \sim p(y)$ and $\theta \sim p(\theta \mid y)$, giving us a free posterior sample. Together, these two facts allow us to modify the framework proposed in Grosse et al. (2015), which starts with a single posterior sample and draws from a sequence of distributions tempered backwards towards the prior, and then estimates an upper bound on $\log p(y)$ accordingly.

This approach yields *reverse-annealed sequential Monte Carlo* (RA-SMC), an algorithm that starts with a single posterior sample and draws from a sequence of distributions tempered backward towards the prior. Unlike Grosse et al. (2015), which sandwiches the true value of $\log p(y)$, RA-SMC directly provides practical EIG estimates and remains robust to overestimating under poor MCMC mixing. We demonstrate this estimator on a coupled spring-mass system, Johnson-Cook model of plastic deformation, and a sequential source location problem–all with multimodal posteriors. Not only do we show that traditional SMC estimators can be used with an order of magnitude fewer particles, but also that our reverse estimator provides a further fourfold improvement in computational cost.

2 Related Work

EIG estimation in BOED has been approached with various methods. *Nested Monte Carlo* (NMC) uses inner-outer loops (Ryan, 2003; Beck et al., 2018) but scales pooorly and has slow-decaying bias (Rainforth et al., 2018; Zheng et al., 2018). *Variational* approaches optimize an approximate posterior (Dahlke et al., 2023; Foster et al., 2019, 2020); they scale better but can be costly and miss complex posterior structure (Pacheco & Fisher, 2019). *Likelihood-free* methods bypass liekelihood via density-ratio estimation, as in LFIRE (Kleinegesse et al., 2021), or by directly learning the objective, as in MINEBED (Kleinegesse & Gutmann, 2020). For sequential design, *reinforcement learning* can learn a design policy (Huan & Marzouk, 2016; Foster et al., 2021; Ivanova et al., 2021; Blau et al., 2022).

Asymptotically consistent alternatives include tempering methods like *annealed importance sampling* (AIS) (Neal, 1996). *Sequential Monte Carlo* (SMC) extends this by resampling and rejuvenating particles along the temperature sequence (Chopin et al., 2020; Del Moral et al., 2006), which has been used for evidence estimation (Xie et al., 2011) and BOED (Ryan et al., 2016). We note here that in this work, "sequential" refers to the progression of particles through a sequence of tempered distributions, as distinct from the temporal sequence in state-space and filtering applications. Our estimator is a single-particle, zero-resample instance of SMC tempering. Unlike AIS, our particle is equally weighted at each temperature and rejuvenated via MCMC, making it conceptually closer to MCMC.

Bidirectional Monte Carlo (BDMC) (Grosse et al., 2015, 2016) runs forward and reverse annealing to produce stochastic upper and lower bounds on $\log p(y)$a. A reverse pass starts from an exact posterior sample and a forward pass from the prior, "sandwiching" the marginal likelihood for model comparison. We adopt BDMC's use of a free posterior draw and reverse anneal but omit the forward pass and bounding machinery.

Our estimator can be regarded as a modification of the BDMC framework for the BOED context. While BDMC "sandwiches" the marginal likelihood, we repurpose the reverse-annealing pass the create a practical EIG estimator. Crucially, we use the thermodynamic integral instead of BDMC's stepping stone algorithm to mitigate the bias of reverse estimators. Furthermore, while BDMC requires many particles for tight bounds, our analysis of EIG's variance structure shows a single particle provides sufficient accuracy at a fraction of the compuational cost. To our knowledge, this is a novel application of reverse-annealed SMC to BOED and constitutes a new EIG estimator.

The methods described above present a diverse set of trade-offs between computational cost, scalability, and asymptotic guarantees. This work specifically focuses on improving the efficiency of tempering-based Monte Carlo estimators, like AIS and SMC, which provide asymptotically-exact estimates crucial for high-fidelity applications, and we show that the RA-SMC estimator makes this powerful but expensive class of methods more practical. To that end, we first review the standard SMC framework, which forms the basis of our proposed approach.

3 Preliminaries: Annealed Sequential Monte Carlo

We briefly review the SMC framework (Chopin et al., 2020) and the SMC-based stepping stone algorithm (Xie et al., 2011) that is commonly used for computing model evidence $p(y)$. SMC evolves a population of N particles from a simple initial distribution (e.g., the prior) to the posterior. It does so by progressing through a sequence of intermediate tempered distributions using importance resampling and Markov chain Monte Carlo (MCMC) steps. One commonly-chosen sequence of tempered distributions is the power posterior sequence (Friel & Pettitt, 2008):

$$p_{t_i}(\theta \mid y) = \frac{p(y \mid \theta)^{t_i} p(\theta)}{z_{t_i}(y)}, \quad \text{where,} \quad z_{t_i}(y) = \int_\theta p(y \mid \theta)^{t_i} p(\theta)\, \mathrm{d}\theta \tag{3}$$

and $0 = t_0 \le \cdots \le t_N = 1$ is an increasing sequence of temperatures. The lowest temperature t_0 recovers the prior, and at the highest temperature t_N, the posterior. At each level, we can compute:

$$E[p(y \mid \theta)^{\Delta t_i}] = \int_\theta p(y \mid \theta)^{\Delta t_i} \frac{p(y \mid \theta)^{t_i} p(\theta)}{z_{t_i}}\, \mathrm{d}\theta = \frac{\int_\theta p(y \mid \theta)^{t_{i+1}} p(\theta)\, \mathrm{d}\theta}{z_{t_i}} = \frac{z_{t_{i+1}}(y)}{z_{t_i}(y)} \tag{4}$$

where $\Delta t_i = t_{i+1} - t_i$. Taking the product up to the $N-1$ level yields the marginal likelihood $p(y)$:

$$\prod_{i=0}^{N-1} \frac{z_{t_{i+1}}(y)}{z_{t_i}(y)} = \frac{z_{t_1}(y)}{z_{t_0}(y)} \frac{z_{t_2}(y)}{z_{t_1}(y)} \cdots \frac{z_{t_N}(y)}{z_{t_{N-1}}(y)} = \frac{z_{t_N}(y)}{z_{t_0}(y)} = \frac{p(y)}{1}. \tag{5}$$

This is known as the stepping-stone algorithm (Xie et al., 2011), and in SMC the number of levels and their temperatures can be chosen adaptively (Catanach & Beck, 2018). The tempering gradually guides the samples to areas of high posterior density, and leads to some of the most accurate estimates of $p(y)$ (Fourment et al., 2020) via the following estimator:

$$\hat{p}(y) = \prod_{i=0}^{N-1} \frac{1}{N} \sum_{j=1}^{n} p(y \mid \theta_{i,j})^{\Delta t_i}, \qquad \text{where } \{\theta_{i,j}\}_{j=1}^{n} \sim p_{t_i} \tag{6}$$

4 Reverse Annealed Sequential Monte Carlo

4.1 Motivation: Balancing Variances

In BOED we are not interested in solely estimating $p(y)$; we are interested in EIG(d), for which the individual IG(y) will depend on their own $p(y)$. Hence, for an estimate of the EIG there are two sources of variance. The first is variance in $\mathrm{IG}(y)$ across the datasets y, and the second is variance from its estimate $\mathrm{I\hat{G}}(y)$ for a given y, which we denote $\mathrm{Var}(\mathrm{I\hat{G}}(y) \mid y)$. If we assume $\mathrm{Var}(\mathrm{I\hat{G}}(y) \mid y)$ is constant across y and $\mathrm{I\hat{G}}$ is unbiased, we can formalize this through the law of total variance:

$$\mathrm{Var}(\mathrm{I\hat{G}}(y)) = \mathbb{E}[\mathrm{Var}(\mathrm{I\hat{G}}(y) \mid y)] + \mathrm{Var}(\mathbb{E}[\mathrm{I\hat{G}}(y) \mid y]) = \mathrm{Var}(\mathrm{I\hat{G}}(y) \mid y) + \mathrm{Var}(\mathrm{IG}(y)) \tag{7}$$

Our experiments find that SMC can be overly precise in the sense that $\mathrm{Var}(\mathrm{I\hat{G}}(y) \mid y) \ll \mathrm{Var}(\mathrm{IG}(y))$. Significant cost is spent on achieving excellent information gain estimates for each dataset, but this precision is unwarranted in light of the overall variance across datasets. As an example, we demonstrate this on the coupled spring-mass system of Sec. 5.1. For a fixed design, we draw 100 different y using different θ, and for each we compute 30 estimates $\mathrm{I\hat{G}}(y)$ using an SMC algorithm (Catanach & Beck, 2018) with 250 particles. The results are summarized in Table 1a, where we find that the variance of $\mathrm{I\hat{G}}(y)$ is two orders of magnitude less than $\mathrm{Var}(\mathrm{IG}(y)) = 22.4$.

Dataset	$\mathrm{IG}(y_i)$	$\mathrm{Var}(\mathrm{I\hat{G}}(y_i) \mid y_i)$
y_1	20.71	0.059
y_{51}	11.40	0.039
y_{60}	19.24	0.093
y_{71}	23.39	0.110
y_{100}	11.57	0.021

(a)

# Particles	$\mathrm{IG}(y_1)$	$\mathrm{Var}(\mathrm{I\hat{G}}(y_i) \mid y_i)$
250	20.210	0.081
150	20.377	0.133
50	20.513	0.570
20	20.399	1.384
10	24.802	25.123

(b)

Table 1: (a) Selected variances of thirty SMC estimates of IG (250 particles). The variance of IG across all 100 datasets is 22.4. Full results in Figure 10 (appendix). (b) Comparison of $\mathrm{Var}(\mathrm{I\hat{G}}(y_1) \mid y_1)$ for different numbers of SMC particles.

We modulate the variance of the forward SMC estimator by reducing the number of particles. Shown in Table 1b, we find that reducing particles from 250 to 20 still yields estimators with an order of magnitude less variance than $\mathrm{Var}(\mathrm{IG}(y))$. Only when we get to 10 particles does $\mathrm{Var}(\mathrm{I\hat{G}}(y)) \approx \mathrm{Var}(\mathrm{IG}(y))$. These few-particle SMC estimators are no longer useful for estimating individual $\mathrm{IG}(y)$ due to their variance and thus could not be applied in other contexts–their utility is unique to calculating EIGs.

Single particle estimates We now consider the extreme case of using only a single particle. This seems ill-advised, however failure is a consequence of poor MCMC mixing, not failure of estimation using few samples. To show this, we consider whether we can use a single sample from a well-mixed Markov chain at each temperature. To ensure proper mixing we run forward SMC using 1000 particles, but estimate IG using only a single random particle from each temperature. This results in a variance of 14.903, which is roughly half $\mathrm{Var}(\mathrm{IG}(y))$. This demonstrates that a single particle IG estimate, from a well-mixed chain, is feasible for experimental design. To obtain such a result we temper backwards, from the posterior to the prior distribution, which we discuss next.

4.2 Reverse-annealed SMC Algorithm

Now we make use of a second unique feature of BOED: datasets are simulated when computing the EIG. This means that we have access to the true underlying parameter θ^*. Crucially, we can treat each joint sample (y, θ^*) as being generated first by drawing y from its marginal, and then θ^* from the posterior. This gives us one *free* draw from the posterior, and so we can start SMC sampling from θ^* and consider sampling a sequence of tempered distributions beginning from the posterior and going to the prior, taking a single sample at each level. This simplifies sampling as we start with a sample from the most difficult distribution and decrease temperature over time, preventing degeneracy issues where our samples end up stuck in low likelihood regions.

We call this scheme *reverse-annealed SMC* (RA-SMC). Since we will be increasing the variance in our estimates, we use the thermodynamic integral (Gelman & Meng, 1998) to help reduce bias by directly targeting $\log p(y)$:

$$\log p(y) = \int_0^1 \int_\theta \log p(y \mid \theta) \frac{p(y \mid \theta)^t p(\theta)}{z_t(y)} \, \mathrm{d}\theta \, \mathrm{d}t. \tag{8}$$

A proof of this identity is provided in Appendix A.1.

Algorithm 1 Reverse annealed sequential Monte Carlo

```
Require: Dataset $(\theta^*, y)$, Temperatures $t = \{t_0, \ldots, t_N\}$
Ensure: Output $\hat{\mathrm{IG}}(y)$
Initialize $\theta \leftarrow \theta^*$, $i \leftarrow N-1$, $l \leftarrow Array[\log p(y \mid \theta^*)]$
while $i \geq 0$ do
    $\theta \leftarrow MCMC(\theta, p_{t_i})$                    { Run MCMC on $p_{t_i}$ starting at $\theta$}
    $i \leftarrow i - 1$
    $l$.append($\log p(y \mid \theta)$)
end while
return $\log p(y \mid \theta^*) - Simpson(t, l)$        { Use Simpson's rule for thermodynamic integral.}
```

The temperature sequence provides a discretization of t on $[0, 1]$, and we then use Simpson's rule (Young & Gregory, 2012) to approximate the outer integral (Calderhead & Girolami, 2009). At each tempering level, the particle is advanced via MCMC runs targeting $p_{t_i}(\theta \mid y)$, which is then used in evaluating the thermodynamic integral. By interchanging the order of integration, we can also view our estimator as first doing numerical integration with Simpson's rule using a single draw at each temperature, and then averaging over all the integrals. This enables us to estimate Monte Carlo standard errors by computing the variance across the integrals. The full RA-SMC estimator is thus defined as follows.

Definition 4.1. *For a fixed y and design d, define*

$$\hat{\ell}_i^{(M)}(y, d) = \log p(y \mid \theta_i^{(M)}, d)$$

and

$$\widehat{\log p}_{N,M}(y, d) = S_N(\hat{\ell}_0^{(M)}(y, d), \hat{\ell}_1^{(M)}(y, d), \ldots, \hat{\ell}_N^{(M)}(y, d)).$$

Here, $\theta_i^{(M)}$ denotes a sample drawn from an M-step MCMC sampler targeting p_{t_i} as its stationary distribution, and S_N is the composite 1/3 Simpson's rule estimator of the input integral evaluated at $N+1$ temperature levels $t_i = (i/N)$, $i, = 0, 1, \ldots, N$. Then the RA-SMC estimator *for design d is:*

$$\widehat{EIG}(d) = \frac{1}{K} \sum_{k=1}^{K} \log p(y_k \mid \theta_k) - \widehat{\log p}_{N,M}(y_k, d), \qquad \textit{where } \{(y_k, d_k)\}_{k=1}^{K} \overset{iid}{\sim} p(y, \theta)$$

We now establish a main property of RA-SMC–it is an asymptotically unbiased estimator of EIG:

Lemma 4.2. *Define the RA-SMC estimator as in Definition 4.1. If the MCMC sampler used to draw each $\theta_i^{(M)}$ defines an ergodic Markov chain with stationary distribution p_{t_i}, and if $\mathbb{E}_{p_t}[\log p(y \mid \theta)]$ is four times continuously-differentiable for all $t \in [0, 1]$, then the RA-SMC estimator is asymptotically unbiased.*

The proof of Lemma 4.2, which can be found in full in Appendix A.1, relies on the asymptotic convergence of the composite Simpson's rule estimator as well as the convergence to the correct stationary distribution of a valid MCMC sampler.

The thermodynamic integral approach is also valid for forward SMC, but the number of tempering levels needed for accurate integration tends to be higher than the number of tempering levels needed for good SMC estimates, and the bias is less of an issue when the estimate of $p(y)$ is precise. The full algorithm is presented in Algorithm 1, and despite only using a single sample at each iteration, we will see in Section 5 that its accuracy is comparable to forward SMC with far more particles.

5 Experimental Results

We compare our algorithm to the forward SMC algorithm of Catanach & Beck (2018), which adaptively chooses the tempering levels and MCMC iterations based on effective sample size calculations. Different numbers of particles are also considered to illustrate the discussion in Section 4.1, with a 250 particle run considered the gold standard against which we compare. For our backward estimator, we use a fixed tempering sequence based on Calderhead & Girolami (2009), with $N = 100$ levels and temperatures $t_i = (i/N)^5$ (see Corollary A.1). For the MCMC kernel we use a simple random walk

Metropolis, where the proposal standard deviation is adapted based on the previous temperature's acceptance rate using the feedback controller of Catanach (2017) to target an ideal acceptance rate of 0.234 (Gelman et al., 1997). Based on an analysis shown in Appendix A.2.1, we fix the number of tempering levels at 100 and only adjust the number of MCMC iterations per temperature for simplicity. We implement an early stopping criterion for MCMC at each level once the Spearman correlation between the starting log likelihoods and the current log likelihoods drops below 0.1. We also halve the number of steps taken once the proposal standard deviation equals the prior standard deviation, indicating that the power posterior is diffuse enough such that more iterations are not critical.

We observe better performance with fewer MCMC iterations across almost all configurations, though overestimation is now more likely. For tuning, we fix a design and run multiple MCMC iterations, stopping roughly when our estimates stabilize while accounting for Monte Carlo standard error, which ended up being 60 iterations. Any initial SMC runs used to determine whether this sampler is viable as mentioned in Section 4.1 can also be used to inform tuning.

5.1 Coupled spring-mass system

We first explore a coupled spring-mass system depicted in Fig. 1. Two masses, m_1 and m_2, are on a surface with respective friction coefficients b_1 and b_2 and joined by a spring with spring constant k_2. The first mass then joined to a fixed point by a second spring with spring constant k_1. The springs are assumed to have length 0 when no forces are applied to them, and the starting positions and velocities of the masses are set to 0. Each of the two masses, their friction coefficients, and the two spring constants are considered unknown parameters, so the posterior is 6D: $(m_1, m_2, b_1, b_2, k_1, k_2)$. All parameters have log-normal priors with mean 0 and SD 1. The experiment imparts a damped oscillating force on the system representing a vibration, given by:

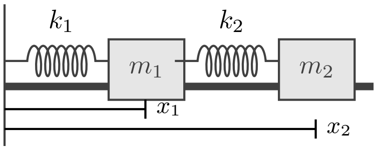

Figure 1: Coupled spring-mass system. Each of the masses also has an friction coefficient b_1 and b_2.

$$x_1' = v_1, \quad x_2' = v_2, \quad v_1' = \frac{-b_1 v_1 - (k_1 + k_2)x_1 + k2x_2}{m_1}, \quad v_2' = \frac{-b_2 v_2 + k_2(x_1 - x_2) + f(\gamma, t)}{m_2}$$

where $f(\gamma, t) = 5\sin(\gamma t)\exp(-t/5)$ is the forcing function, x_i is the position of the ith mass, and v_i is the velocity of the ith mass. We observe a noisy position x_1 at 100 equally spaced time points. The noise is Gaussian with mean 0 and SD 0.025, with observed data $y = \{y_1, \ldots, y_{100}\}$ and,

$$y_t = x_{1t} + \epsilon_t, \quad \epsilon_t \overset{iid}{\sim} N(0, 0.025^2), \quad t = 1, \ldots, 100$$

where x_{1t} is the position of the first mass at time t. Fig. 2 shows three randomly generated datasets. We consider ten equally spaced designs γ between 0 and 2 of the form $0.2j, j = 1, \ldots, 10$. By observing only one mass, we induce multimodality and curvature in the posterior distribution. Fig. 3 shows four dimensions of an example posterior. 1000 datasets are drawn for each method, with performance measured by the number of likelihood evaluations required and how well the final EIG values correspond to those of an expensive forward SMC run. Likelihood evaluations are the dominant cost and are therefore used as a hardware agnostic metric for computational efficiency.

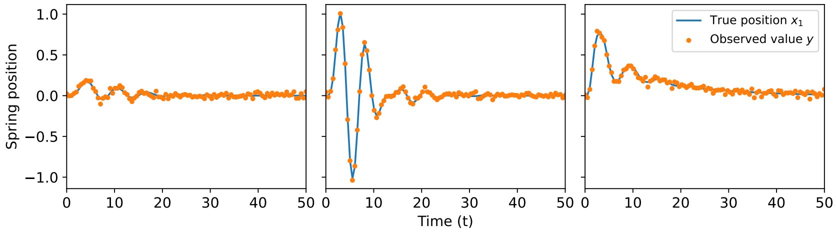

Figure 2: Three examples of observed data y in orange, along with the true signal x in blue for the spring-mass model. The true signal corresponds to the position of the first mass m_1 between time $t = 0$ and $t = 50$, and is observed over 100 equally-spaced time points.

Magnetic reverse-annealed SMC steps To aid MCMC mixing we use knowledge of the target distribution (the prior), when tempering backwards, to inform the initialization at each level. The idea is that the next temperature level should place more mass towards the prior. Hence, instead of starting θ at the last position of the previous level, we nudge the starting point of the MCMC towards the prior mean. Between levels, we take up to a tenth of the planned MCMC iterations toward the prior mean using the proposal standard deviation as the step size, stopping if the log likelihood at any new step is less than a tenth of the starting log likelihood. We note that this is an optional enhancement, rather than a core component of the method.

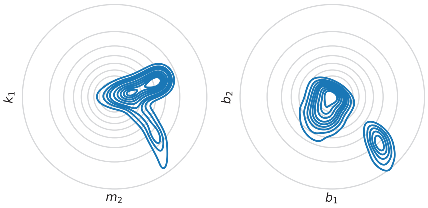

Figure 3: Example spring-mass posterior for four of the parameters based on kernel density estimation using samples from 250-particle forward SMC, with the standard normal priors shown in grey. The posterior demonstrates multimodality and curvature.

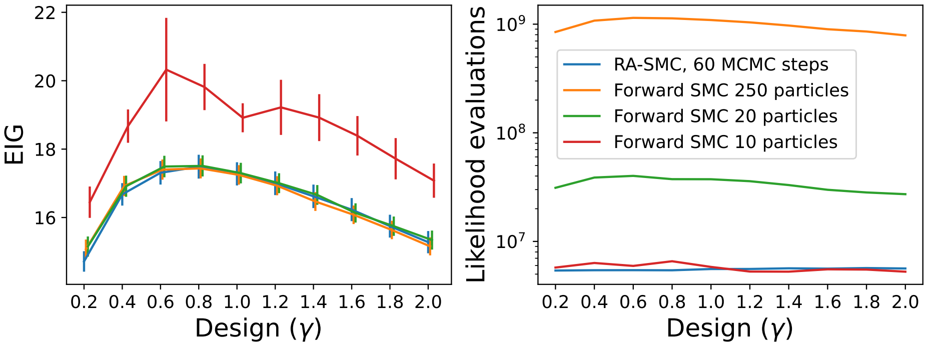

Figure 4: Left: EIG estimates across 10 designs of the spring-mass model, with vertical bars representing two Monte Carlo standard errors above and below the estimate. Right: Number of likelihood evaluations for each estimate. The adaptive nature of forward SMC results in a varying number of evaluations per design.

Results A comparison of the EIG curves resulting from traditional forward SMC estimators with varying numbers of particles to the backward SMC estimator's EIG curve is shown in Figure 4. By decreasing the number of forward SMC particles by an order of magnitude to 20, we gain an order of magnitude of efficiency with little loss of performance compared to the gold standard 250 particle runs. At 10 particles, significant upward bias and noise occurs. Notably, the failure is catastrophic as opposed to gradual; below some threshold, mixing fails and the estimates are poor, while above that threshold the estimates are still stable. Our reverse estimator performs well with another fourfold decrease in likelihood evaluations compared to the 20 particle forward SMC.

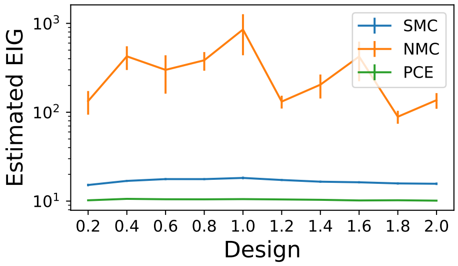

Figure 5: Estimated expected information gain (EIG) for the springmass design problem across design values from 0.2 to 2.0. Each curve corresponds to a different estimator: Forward SMC, Nested Monte Carlo (NMC), and Prior Contrastive Estimation (PCE). Error bars indicate estimator standard errors, computed across replicates. SMC estimates use 100 outer samples and 20 particles per stage; NMC and PCE estimates use 100 outer samples and 300,000 inner samples. Error bars for the SMC and PCE curves are present but too small to be visible.

Other Monte Carlo Baselines As a baseline, we also evaluated Nested Monte Carlo (NMC) and Prior Contrastive Estimation (PCE) on the spring-mass problem, allocating the same computational budget as the 20-particle forward SMC run. As shown in Figure 5, both estimators performed poorly. NMC produced inaccurate estimates with large standard errors, while PCE exhibited a strong downward bias and failed to locate the optimal design. Since the data are informative, the resulting posterior is sharply peaked. The prior-based sampling of these methods is inadequate to explore this region, which leads to unstable and biased evidence estimation.

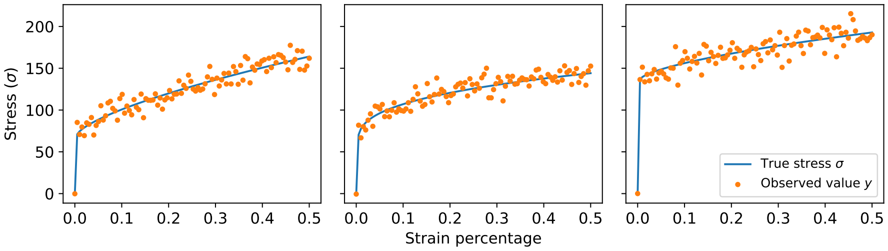

Figure 6: Three examples of observed data y in orange, along with the true signal σ in blue for the Johnson-Cook model. The true signal corresponds to the output stress of a material for strain percentage ε between 0 and 0.5, observed at 100 equally spaced values.

5.2 Johnson-Cook model

We run a Johnson-Cook model of a stress-strain curve for a hypothetical material under plastic deformation. The data follows the following model, where the experiment involves observing the stress at 100 equally spaced strain percentages ε from 0 to 0.5, with varying measurement noise dependent on whether the material is in the elastic or plastic phase:

$$y = \begin{cases} E\varepsilon + \delta_e & \text{if } \varepsilon E < A \\ \left(A + B\left(\varepsilon - \frac{A}{E}\right)^n\right) \times (1 + C\log(\dot{\varepsilon})) \times \left(1 - \left(\frac{T - 293}{775 - 293}\right)^m\right) + \delta_p & \text{otherwise,} \end{cases}$$

where $\delta_e \overset{iid}{\sim} N(0, 1)$ and $\delta_p \overset{iid}{\sim} N(0, 10)$. We consider the strain rate $\dot{\varepsilon}$ and temperature T as experimental variables. Other parameters are unknown material constants with the following priors:

$$E \sim \mathcal{N}(73000, 10000^2), \quad A \sim \mathcal{N}(350, 100^2), \quad B \sim \mathcal{N}(650, 200^2),$$
$$C \sim \text{Beta}(2, 10), \quad n \sim \text{Beta}(2, 5), \quad m \sim \text{Beta}(2, 5).$$

Figure 6 shows examples of three randomly generated datasets for $\dot{\varepsilon} = 0.1$ and $T = 300$. For simplicity, we evaluate five strain rates $\{0.001, 0.005, 0.01, 0.05, 0.1\}$ for the same temperature 300, and then multiple temperatures $\{300, 400, 500, 600, 700\}$ for the same strain rate 0.1. For the MCMC kernel, we use a proposal standard deviation equal to the prior standard deviations scaled to target the 0.234 acceptance rate, though no adaptation of the proposal to the prior is done since the prior is not multivariate Gaussian. Similarly to the coupled spring-mass model in Section 5.1, we use 1000 datasets with 60 MCMC steps as well as the magnetic SMC steps.

Results Figure 7 displays the EIG curves resulting from forward SMC estimators with different population sizes compared to the EIG curve generated by the reverse-annealed SMC estimator with varying MCMC iterations when using both strain rate and temperature as the design variable. Similarly to the spring-mass model, we see that we can decrease the number of particles to 20 without significant impact to the EIG curve in both cases. We also find that the reverse-annealed SMC estimator with 60 MCMC steps achieves good results. Moreover, the computation budget for either configuration is roughly equivalent to forward SMC with 10 particles, while yielding substantially more accurate EIG estimates.

Unlike with the spring-mass model, the reverse-annealed SMC estimator with 10 MCMC steps is not as heavily biased downward, providing a better estimator than the 10-sample forward SMC estimator and requiring an order of magnitude fewer likelihood evaluations. When using temperature as the design variable, the EIG curve from the reverse-annealed SMC estimator matches the “true” EIG curve even better than when using strain rate as the design. Unsurprisingly, we still see a higher standard error than reverse-annealed SMC with 60 MCMC steps, although the standard error is lower in the temperature design setting than in the strain-rate design setting.

5.3 Source Finding

Finally, we apply our reverse-annealed SMC estimator to the source-localization problem described in Foster et al. (2021), in which two hidden sources emit a signal whose intensity decays according to the inverse-square law. At each step, a sensor placed at a design location ξ, records a noisy measurement of the aggregate signal intensity. The objective is to sequentially choose sensor placements $\{\xi_t\}_{t=1}^T$

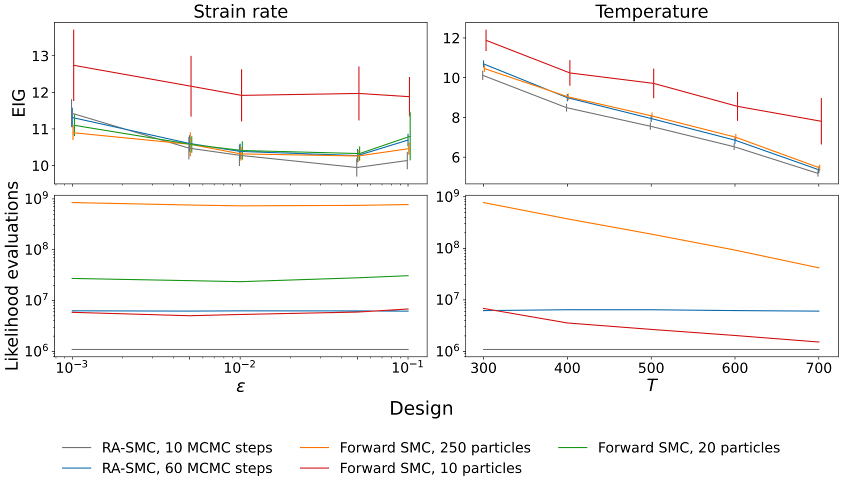

Figure 7: EIG and computational cost results for different under two different choices of design variable for the Johnson-Cook model. Left column: EIG and computational cost for five choices of strain rate at a fixed temperature 300. Reverse-annealed SMC yields accurate EIG curves with orders of magnitude fewer likelihod evaluation compared to forward SMC baselines. Right column: EIG and computational cost results for five choices of temperature at a fixed strain rate 0.1. Here, forward SMC is able to effectively adapt the number of iterations required at the higher temperatures. Error bars indicate two Monte Carlo standard errors.

to efficiently infer the unknown source coordinates θ from the noisy observations $\{y_t\}_{t=1}^{T}$. The noiseless observation model is:

$$\mu(\theta, \xi) = b + \sum_{k=1}^{K} \frac{1}{m + \|\theta_k + \xi\|^2},$$

where $b, m > 0$ are constants that control background and maximum signal, respectively. We observe the log intensity, and use the following prior and likelihood models:

$$\theta_k \overset{\text{iid}}{\sim} \mathcal{N}(0, I_2), \quad \log y \mid \theta, \xi \sim \mathcal{N}(\log \mu(\theta, \xi), \sigma).$$

Each observation is chosen by selecting: $\xi_t = \arg\max_{\xi} \text{EIG}(\xi \mid y_{1:t-1}, \xi_{1:t-1})$. Once ξ_t is chosen, the observer records y_t, the posterior is updated to $p(\theta \mid y_{1:t}, \xi_{1:t})$, and the design-measure-update cycle is repeated until a terminal time T is reached.

In our experiments we choose $m = 10^{-4}$ and $b = 10^{-1}$, matching the values used in Foster et al. (2021), and we restrict observation locations to a 20×20 grid covering the square domain $[-3, 3] \times [-3, 3]$. We perform $T = 15$ steps of sequential optimization using RA-SMC and forward SMC with 50 and 100 particles.

Results Figure 8 shows the results of the source-finding problem using reverse-annealed SMC and forward SMC with 50 and 100 particles. We find that reverse-annealed SMC not only produces tightly clustered sensor placements around the true sources, but does so with substantially less computation. Over 15 measurements, reverse-annealed SMC required 8.4×10^9 likelihood evaluations, whereas forward SMC consumed about 3.7×10^{10} and 4.8×10^{10} evaluations for 50 and 100 particles, respectively.

Despite this reduction in evaluation cost, reverse-annealed SMC yields better convergence than 50-particle forward SMC and similar performance to 100-particle forward SMC. Figure 9 shows the KL divergence between the prior and the posterior at each iteration of the sequential design process. We see that RA-SMC performs similarly to 100-particle forward SMC, while 50-particle forward SMC gives erratic results.

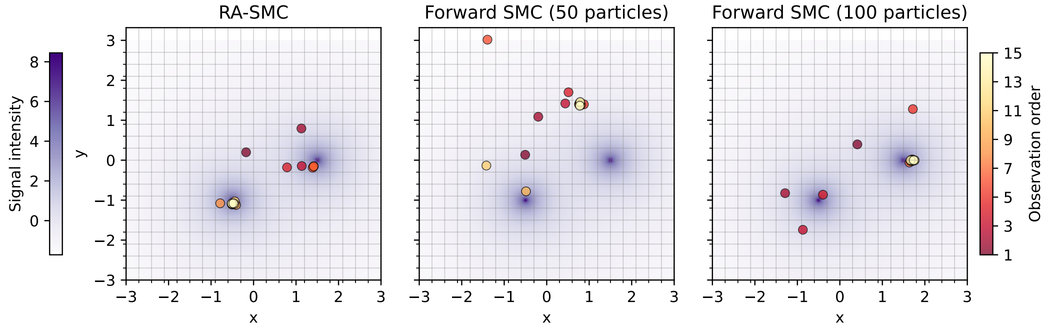

Figure 8: Side-by-side comparison of sequential sensor placements for source localization using reverse-annealed SMC (left), forward SMC with 50 particles (middle) and forward SMC with 100 particles (right). The background heatmap indicates the log-signal intensity over the domain, and each marker shows a sensor location colored by its observation order (dark to light). Reverse-annealed SMC and 100-particle SMC rapidly concentrate measurements near the true source positions, whereas 50-particle forward SMC exhibits a more dispersed sampling pattern. The likelihood evaluations were 8.4×10^9, 3.7×10^{10}, and 4.8×10^{10}, respectively.

5.4 Discussion and Limitations

The single-particle, reverse trajectory of RA-SMC has key limitations. It complicates adaptive MCMC proposals and tempering schedules, which often require population statistics. Poor MCMC mixing when annealing from a peaked posterior toward the flatter prior can yield conservative IG estimates. Determining its suitability for a problem is currently ad hoc, requiring preliminary runs to find efficiency gains. A robust diagnostic for this would therefore be valuable.

On the other hand, because RA-SMC initializes from a true posterior sample, it may be less susceptible to the particle degeneracy issues that hinder traditional multi-particle SMC methods in high dimensions. Future research could explore developing diagnostics to assess estimator suitability, incorporating more sophisticated MCMC kernels (e.g., Hamiltonian Monte Carlo (Neal, 2012) or the No-U-Turn sampler (Hoffman et al., 2014)), studying the method's scalability in high dimensions, devising adaptive strategies using multiple particles to improve both MCMC mixing and the selection of tempering levels, extending the framework to real-world data by initializing the reverse trajectory with approximate posterior draws from likelihood-free methods, and conducting a more extensive comparison to other estimators for BOED.

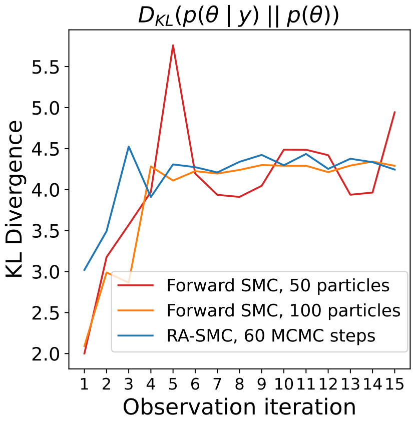

Figure 9: Evolution of the KL divergence over 15 sequential observations for forward SMC with 50 particles (red), forward SMC with 100 particles (orange), and reverse-annealed SMC with 60 MCMC steps (blue). RA-SMC converges as smoothly and rapidly as 100-particle forward SMC, while 50-particle forward SMC yields more erratic KL divergence estimates.

Acknowledgments and Disclosure of Funding

Sandia National Laboratories (SNL) is a multimission laboratory managed and operated by National Technology & Engineering Solutions of Sandia, LLC, a wholly owned subsidiary of Honeywell International Inc., for the U.S. Department of Energy's National Nuclear Security Administration under contract DE-NA0003525. SAND#2025-13387C. Initial research was supported by SNL Laboratory Directed Research and Development. This paper describes objective technical results and analysis. Any subjective views or opinions that might be expressed in the paper do not necessarily represent the views of the U.S. Department of Energy or the United States Government.

References

Beck, J., Dia, B. M., Espath, L. F., Long, Q., and Tempone, R. Fast bayesian experimental design: Laplace-based importance sampling for the expected information gain. *Computer Methods in Applied Mechanics and Engineering*, 334:523–553, 2018. ISSN 0045-7825. doi: https://doi.org/10.1016/j.cma.2018.01.053. URL https://www.sciencedirect.com/science/article/pii/S0045782518300616.

Blau, T., Bonilla, E. V., Chades, I., and Dezfouli, A. Optimizing sequential experimental design with deep reinforcement learning. In Chaudhuri, K., Jegelka, S., Song, L., Szepesvari, C., Niu, G., and Sabato, S. (eds.), *Proceedings of the 39th International Conference on Machine Learning*, volume 162 of *Proceedings of Machine Learning Research*, pp. 2107–2128. PMLR, 17–23 Jul 2022. URL https://proceedings.mlr.press/v162/blau22a.html.

Calderhead, B. and Girolami, M. Estimating Bayes factors via thermodynamic integration and population MCMC. *Computational Statistics & Data Analysis*, 53(12):4028–4045, 2009.

Catanach, T. A. *Computational methods for Bayesian inference in complex systems*. California Institute of Technology, 2017.

Catanach, T. A. and Beck, J. L. Bayesian updating and uncertainty quantification using sequential tempered MCMC with the rank-one modified Metropolis algorithm. *arXiv preprint arXiv:1804.08738*, 2018.

Chopin, N., Papaspiliopoulos, O., et al. *An introduction to sequential Monte Carlo*, volume 4. Springer, 2020.

Dahlke, C., Zheng, S., and Pacheco, J. Fast variational estimation of mutual information for implicit and explicit likelihood models. In *International Conference on Artificial Intelligence and Statistics*, pp. 10262–10278. PMLR, 2023.

Del Moral, P., Doucet, A., and Jasra, A. Sequential monte carlo samplers. *Journal of the Royal Statistical Society Series B: Statistical Methodology*, 68(3):411–436, 2006.

Foster, A., Jankowiak, M., Bingham, E., Horsfall, P., Teh, Y. W., Rainforth, T., and Goodman, N. Variational bayesian optimal experimental design. *Advances in Neural Information Processing Systems*, 32, 2019.

Foster, A., Jankowiak, M., O'Meara, M., Teh, Y. W., and Rainforth, T. A unified stochastic gradient approach to designing bayesian-optimal experiments. In Chiappa, S. and Calandra, R. (eds.), *Proceedings of the Twenty Third International Conference on Artificial Intelligence and Statistics*, volume 108 of *Proceedings of Machine Learning Research*, pp. 2959–2969. PMLR, 26–28 Aug 2020. URL https://proceedings.mlr.press/v108/foster20a.html.

Foster, A., Ivanova, D. R., Malik, I., and Rainforth, T. Deep adaptive design: Amortizing sequential bayesian experimental design. In Meila, M. and Zhang, T. (eds.), *Proceedings of the 38th International Conference on Machine Learning*, volume 139 of *Proceedings of Machine Learning Research*, pp. 3384–3395. PMLR, 18–24 Jul 2021. URL https://proceedings.mlr.press/v139/foster21a.html.

Fourment, M., Magee, A. F., Whidden, C., Bilge, A., Matsen IV, F. A., and Minin, V. N. 19 dubious ways to compute the marginal likelihood of a phylogenetic tree topology. *Systematic biology*, 69 (2):209–220, 2020.

Friel, N. and Pettitt, A. N. Marginal likelihood estimation via power posteriors. *Journal of the Royal Statistical Society Series B: Statistical Methodology*, 70(3):589–607, 2008.

Gelman, A. and Meng, X.-L. Simulating normalizing constants: From importance sampling to bridge sampling to path sampling. *Statistical science*, pp. 163–185, 1998.

Gelman, A., Gilks, W. R., and Roberts, G. O. Weak convergence and optimal scaling of random walk metropolis algorithms. *The annals of applied probability*, 7(1):110–120, 1997.

Grosse, R. B., Ghahramani, Z., and Adams, R. P. Sandwiching the marginal likelihood using bidirectional Monte Carlo, November 2015. URL http://arxiv.org/abs/1511.02543. arXiv:1511.02543 [stat].

Grosse, R. B., Ancha, S., and Roy, D. M. Measuring the reliability of MCMC inference with bidirectional Monte Carlo. In Lee, D., Sugiyama, M., Luxburg, U., Guyon, I., and Garnett, R. (eds.), *Advances in Neural Information Processing Systems*, volume 29. Curran Associates, Inc., 2016. URL https://proceedings.neurips.cc/paper_files/paper/2016/file/0e9fa1f3e9e66792401a6972d477dcc3-Paper.pdf.

Hoffman, M. D., Gelman, A., et al. The No-U-Turn sampler: adaptively setting path lengths in Hamiltonian Monte Carlo. *J. Mach. Learn. Res.*, 15(1):1593–1623, 2014.

Huan, X. and Marzouk, Y. M. Sequential bayesian optimal experimental design via approximate dynamic programming, 2016. URL https://arxiv.org/abs/1604.08320.

Ivanova, D. R., Foster, A., Kleinegesse, S., Gutmann, M. U., and Rainforth, T. Implicit deep adaptive design: Policy-based experimental design without likelihoods. In Ranzato, M., Beygelzimer, A., Dauphin, Y., Liang, P., and Vaughan, J. W. (eds.), *Advances in Neural Information Processing Systems*, volume 34, pp. 25785–25798. Curran Associates, Inc., 2021. URL https://proceedings.neurips.cc/paper_files/paper/2021/file/d811406316b669ad3d370d78b51b1d2e-Paper.pdf.

Kleinegesse, S. and Gutmann, M. U. Bayesian experimental design for implicit models by mutual information neural estimation, 2020. URL https://arxiv.org/abs/2002.08129.

Kleinegesse, S., Drovandi, C., and Gutmann, M. U. Sequential Bayesian Experimental Design for Implicit Models via Mutual Information. *Bayesian Analysis*, 16(3):773 – 802, 2021. doi: 10.1214/20-BA1225. URL https://doi.org/10.1214/20-BA1225.

Lindley, D. V. On a measure of the information provided by an experiment. *The Annals of Mathematical Statistics*, 27(4):986–1005, 1956.

Neal, R. M. Sampling from multimodal distributions using tempered transitions. *Statistics and Computing*, 6(4):353–366, December 1996. ISSN 0960-3174, 1573-1375. doi: 10.1007/BF00143556. URL http://link.springer.com/10.1007/BF00143556.

Neal, R. M. MCMC using Hamiltonian dynamics. *arXiv preprint arXiv:1206.1901*, 2012.

Pacheco, J. and Fisher, J. Variational information planning for sequential decision making. In *The 22nd International Conference on Artificial Intelligence and Statistics*, pp. 2028–2036. PMLR, 2019.

Rainforth, T., Cornish, R., Yang, H., Warrington, A., and Wood, F. On nesting monte carlo estimators. In *International Conference on Machine Learning*, pp. 4267–4276. PMLR, 2018.

Rainforth, T., Foster, A., Ivanova, D. R., and Bickford Smith, F. Modern Bayesian experimental design. *Statistical Science*, 39(1):100–114, 2024.

Ryan, E. G., Drovandi, C. C., McGree, J. M., and Pettitt, A. N. A review of modern computational algorithms for bayesian optimal design. *International Statistical Review*, 84(1):128–154, 2016.

Ryan, K. J. Estimating expected information gains for experimental designs with application to the random fatigue-limit model. *Journal of Computational and Graphical Statistics*, 12(3):585–603, 2003.

Xie, W., Lewis, P. O., Fan, Y., Kuo, L., and Chen, M.-H. Improving marginal likelihood estimation for Bayesian phylogenetic model selection. *Systematic biology*, 60(2):150–160, 2011.

Young, D. and Gregory, R. *A Survey of Numerical Mathematics, Volume I*. Dover Books on Mathematics Series. Dover Publications, Incorporated, 2012. ISBN 9780486145051. URL https://books.google.com/books?id=goSAEYUcMoMC.

Zheng, S., Pacheco, J., and Fisher, J. A robust approach to sequential information theoretic planning. In *International Conference on Machine Learning*, pp. 5941–5949. PMLR, 2018.

A Appendix

A.1 Proofs and additional theory

Proof of Lemma 4.2.

Proof. By the linearity of expectations,

$$
\begin{aligned}
\mathbb{E}[\widehat{\log p}_{N,M}(y,d)] &= S_N(\hat{\ell}_0^{(M)}(y,d), \hat{\ell}_1^{(M)}(y,d), \dots, \hat{\ell}_N^{(M)}(y,d)) \\
&= \mathbb{E}\left[\frac{\Delta t}{3}\left(\hat{\ell}_0^{(M)}(d) + \hat{\ell}_N^{(M)}(d) + 4\sum_{\substack{i=1,\\ i \text{ odd}}}^{N-1} \hat{\ell}_i^{(M)}(d) + 2\sum_{\substack{i=2,\\ i \text{ even}}}^{N-2} \hat{\ell}_i^{(M)}(d)\right)\right] \\
&= \frac{\Delta t}{3}\left(\mathbb{E}[\hat{\ell}_0^{(M)}(d)] + \mathbb{E}[\hat{\ell}_N^{(M)}(d)] + 4\sum_{\substack{i=1,\\ i \text{ odd}}}^{N-1} \mathbb{E}[\hat{\ell}_i^{(M)}(d)] + 2\sum_{\substack{i=2,\\ i \text{ even}}}^{N-2} \mathbb{E}[\hat{\ell}_i^{(M)}(d)]\right).
\end{aligned}
$$

For each i, we have

$$
\lim_{M\to\infty} \mathbb{E}[\hat{\ell}_i^{(M)}(d)] = \mathbb{E}_{p_{t_i}}[\log p(y \mid \theta, d)] := \ell(t_i, y, d),
$$

so

$$
\begin{aligned}
\lim_{M\to\infty} \mathbb{E}[\hat{p}_{N,M}(y,d)] = \frac{\Delta t}{3}&\left(\ell(t_0,y,d) + \ell(t_N,y,d) + 4\sum_{\substack{i=1,\\ i \text{ odd}}}^{N-1} \ell(t_i,y,d) + 2\sum_{\substack{i=2,\\ i \text{ even}}}^{N-2} \ell(t_i,y,d)\right) \\
:= Q_N.&
\end{aligned}
$$

When the fourth derivative is bounded, the composite Simpson rule satisfies the remainder bound:

$$
\left| Q_N - \int_0^1 \ell(t,y,d)\,dt \right| = O(N^{-4}),
$$

so

$$
\lim_{N\to\infty} Q_N = \int_0^1 \ell(t,y,d)\,dt = \int_0^1 \mathbb{E}_{\theta\sim p_t}[\log p(y \mid \theta, d)]\,dt = \log p(y).
$$

Hence,

$$
\lim_{N,M\to\infty} \hat{p}_{N,M}(y,d) = \log p(y \mid d).
$$

Finally, observe that

$$
\begin{aligned}
\lim_{N,M,K\to\infty} \mathbb{E}[\widehat{\text{EIG}}_{N,M,K}(d)] &= \lim_{K\to\infty} \mathbb{E}\left[\frac{1}{K}\sum_{k=1}^{K} \log p(y_k \mid \theta_k, d) - \lim_{N,M\to\infty} \hat{p}_{N,M}(y_k,d)\right] \\
&= \lim_{k\to\infty} \mathbb{E}_{(y,\theta)\sim p(y,\theta)}\left[\log p(y \mid \theta, d) - \lim_{N,M\to\infty} \mathbb{E}[\hat{p}_{N,M}(y,d)]\right] \\
&= \mathbb{E}_{(y,\theta)\sim p(y,\theta)}\left[\log p(y \mid \theta, d) - \log p(y \mid d)\right] \\
&= \text{EIG}(d).
\end{aligned}
$$

Thus, the RA-SMC estimator of $\text{EIG}(d)$ is asymptotically unbiased. □

Corollary A.1. *Under the same conditions as Lemma 4.2, the RA-SMC estimator is asymptotically unbiased for geometrically spaced temperature levels $t_j = (u_j)^c$, where $u_j = j/N$ are uniformly spaced points in $[0,1]$ and $c > 1$ is a constant.*

Proof. We use a standard change of variables. The integral for $\log p(y \mid d)$ is transformed:

$$
\int_0^1 \underbrace{\ell(u^c, y, d) c u^{c-1}}_{:= g(u,y,d)} = \int_0^1 \ell(t,y,d)dt = \log p(y \mid d).
$$

The estimator for $\log p(y \mid d)$ is then constructed by applying the composite Simpson's rule $S_N(\cdot)$ (with uniform step $\Delta u = 1/N$) to MCMC-based estimates $\hat{g}_j^{(M)}(y,d)$ of the transformed integrand $g(u_j; y, d)$. Specifically,

$$\hat{g}_j^{(M)} = c(u_j)^{c-1}\hat{\ell}_j^{(M)}(y,d),$$

where $\hat{\ell}_j^{(M)}(y,d)$ is the MCMC estimate of $\ell((u_j)^c, y, d)$.

The asymptotic unbiasedness argument then applies directly to this estimation of $\int_0^1 g(u,y,d)du$ because of the following two facts. First, the transformed integrand $g(u,y,d)$ is four-times continuously differentiable on $[0,1]$. Second, the MCMC estimates $\hat{g}_j^{(M)}(y,d)$ are asymptotically unbiased in expectation for $g(u_j,y,d)$ as $M \to \infty$: observe that

$$\begin{aligned}\lim_{M\to\infty} \mathbb{E}[\hat{g}_j^{(M)}(y,d)] &= \lim_{M\to\infty} \mathbb{E}[cu^{c-1}\hat{\ell}_j^{(M)}(y,d)] \\ &= \mathbb{E}[cu^{c-1}\ell(t_i,y,d)] \\ &= \mathbb{E}[g(u_i,y,d)].\end{aligned}$$

Under these conditions on the transformed problem, the same $O(N^{-4})$ convergence for the Simpson's rule discretization error (for $g(u)$) and the vanishing MCMC error ensure the asymptotic unbiasedness for estimating $\log p(y \mid d)$ with geometrically spaced temperatures. □

Proof of Equation 8.

Proof. Observe that

$$\begin{aligned}\log p(y) &= \log(z_1(y)) - \log(z_0(y)) \\ &= \int_0^1 \frac{d}{dt}\log(z_t(y))\,dt \\ &= \int_0^1 \frac{1}{z_t(y)}\frac{d}{dt}z_t(y)\,dt \\ &= \int_0^1 \frac{1}{z_t(y)}\frac{d}{dt}\int_\theta p(y \mid \theta)^t p(\theta)\,d\theta\,dt \\ &= \int_0^1 \frac{1}{z_t(y)}\int_\theta \frac{d}{dt}p(y \mid \theta)^t p(\theta)\,d\theta\,dt \\ &= \int_0^1 \frac{1}{z_t(y)}\int_\theta \log p(y \mid \theta)p(y \mid \theta)^t p(\theta)\,d\theta\,dt \\ &= \int_0^1 \int_\theta \log p(y \mid \theta)\frac{p(y \mid \theta)^t p(\theta)}{z_t(y)}\,d\theta\,dt,\end{aligned}$$

as desired. □

A.2 Additional Results

A.2.1 Inner-loop variance vs. outer-loop variance

To validate that $\text{Var}(\hat{\text{IG}}(y) \mid y) \ll \text{Var}(\text{IG}(y))$, we draw 100 datasets y_i, $i = 1, \ldots, 100$ from the spring mass observation model in Sec 5.1. For each of these datasets, we repeatedly compute $\text{IG}(y_i)$ thirty times using forward SMC with 250 particles. Then, we compute $\text{Var}(\hat{\text{IG}}(y) \mid y = y_i)$ across the thirty replicates of $\text{IG}(y_i)$ and compare the estimator variance for a given dataset to that dataset's value of $\text{IG}(y)$. Figure 10 displays this comparison for all 100 datasets. It is clear that the inner-loop estimator variance $\text{Var}(\hat{\text{IG}}(y) \mid y)$ is much smaller than $IG(y)$.

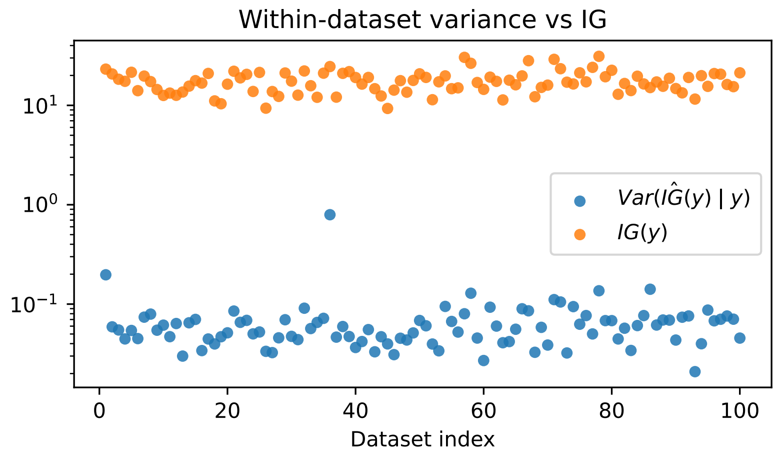

Figure 10: A comparison between Var$(\hat{IG}(y) \mid y)$, the estimator variance from computing IG(y) for a single dataset, and the value of IG(y). We see that Var$(\hat{IG}(y) \mid y)$ is on average two orders of magnitude smaller than IG(y).

A.2.2 Choosing the tempering levels

There is a balance between the number of temperature levels and number of MCMC iterations because more temperatures means that the difference between subsequent distributions is smaller; fewer MCMC iterations should then be required to achieve convergence. Assuming the number of levels is sufficiently large to calculate the thermodynamic integral, it is unclear whether, for example, 100 levels of 100 iterations is generally better than 200 levels of 50 iterations.

Figure 11 demonstrates how the absolute error changes for the model in Section 5.1 as we vary these parameters when compared to a gold standard forward SMC run, and it appears that there is no significant difference past a certain threshold.

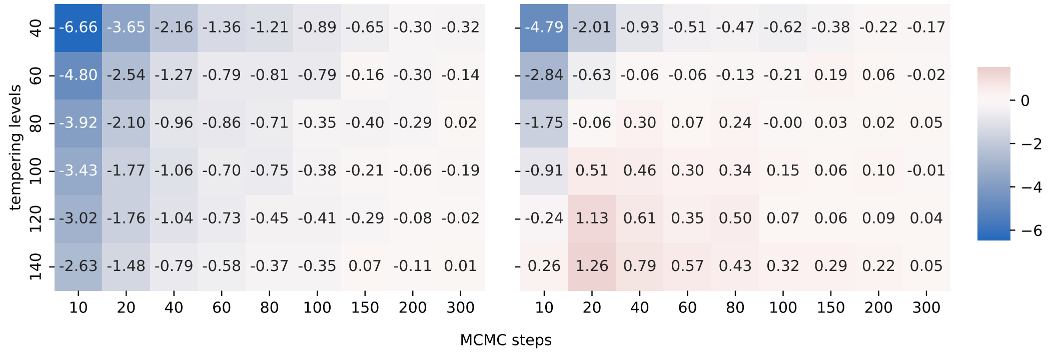

tempering levels	10	20	40	60	80	100	150	200	300
40	-6.66	-3.65	-2.16	-1.36	-1.21	-0.89	-0.65	-0.30	-0.32
60	-4.80	-2.54	-1.27	-0.79	-0.81	-0.79	-0.16	-0.30	-0.14
80	-3.92	-2.10	-0.96	-0.86	-0.71	-0.35	-0.40	-0.29	0.02
100	-3.43	-1.77	-1.06	-0.70	-0.75	-0.38	-0.21	-0.06	-0.19
120	-3.02	-1.76	-1.04	-0.73	-0.45	-0.41	-0.29	-0.08	-0.02
140	-2.63	-1.48	-0.79	-0.58	-0.37	-0.35	0.07	-0.11	0.01

tempering levels	10	20	40	60	80	100	150	200	300
40	-4.79	-2.01	-0.93	-0.51	-0.47	-0.62	-0.38	-0.22	-0.17
60	-2.84	-0.63	-0.06	-0.06	-0.13	-0.21	0.19	0.06	-0.02
80	-1.75	-0.06	0.30	0.07	0.24	-0.00	0.03	0.02	0.05
100	-0.91	0.51	0.46	0.30	0.34	0.15	0.06	0.10	-0.01
120	-0.24	1.13	0.61	0.35	0.50	0.07	0.06	0.09	0.04
140	0.26	1.26	0.79	0.57	0.43	0.32	0.29	0.22	0.05

Figure 11: Left: Absolute error of EIG computed with the standard reverse-annealed SMC, with downward bias trend clearly visible when levels or steps are too low. Right: Error of magnetized reverse-annealed SMC. Values are in comparison to a long 250 particle forward SMC estimate, with Monte Carlo standard errors around 0.3.

A.3 Basic reverse-annealed SMC

We also run a basic version of our estimator with only 10 MCMC iterations for each temperature and no further adaptivity, shown in Figure 12. As expected, this yields underestimates of the EIG. However, the resulting EIG curve can still be used for BOED as the bias is sufficiently similar across designs. The curve is also still relatively smooth due to the lack of degenerate samples increasing the variance. Even if accurate EIG estimates are required, this could be used to enable a coarse first pass to narrow the search space of designs.

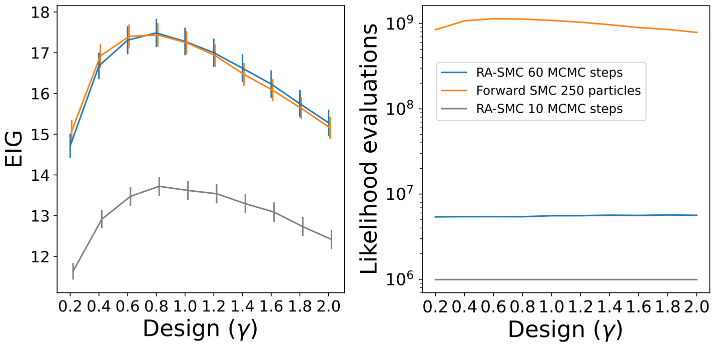

Figure 12: Comparison of results using 10 iterations of MCMC per temperature for reverse-annealed SMC on the spring-mass model. The EIGs are clearly underestimated but still form a usable curve for BOED.

One caveat is that the reverse-annealed SMC has around a 15% higher Monte Carlo standard error, 0.167 vs. 0.145 for forward SMC. This is not surprising since we are increasing $\mathrm{Var}(\hat{\mathrm{IG}}(y) \mid y)$, and so it is reasonable to say that cost of obtaining EIG estimates with the same precision as forward SMC in this case would require about 33% more outer-loop samples than were run in our simulations. However, our main takeaways do not change, as an additional 33% cost is small compared to reduction in inner-loop likelihood evaluations.

NeurIPS Paper Checklist

1. **Claims**

   Question: Do the main claims made in the abstract and introduction accurately reflect the paper's contributions and scope?

   Answer: [Yes]

   Justification: The abstract and introduction accurately state that the paper's primary contribution is a novel EIG estimation method achieving lower computational cost for similar performance across a various BOED problems. These claims are substantiated in the paper's empirical results from several different BOED problems and are supported by a thorough methodological discussion.

   Guidelines:

   - The answer NA means that the abstract and introduction do not include the claims made in the paper.
   - The abstract and/or introduction should clearly state the claims made, including the contributions made in the paper and important assumptions and limitations. A No or NA answer to this question will not be perceived well by the reviewers.
   - The claims made should match theoretical and experimental results, and reflect how much the results can be expected to generalize to other settings.
   - It is fine to include aspirational goals as motivation as long as it is clear that these goals are not attained by the paper.

2. **Limitations**

   Question: Does the paper discuss the limitations of the work performed by the authors?

   Answer: [Yes]

   Justification: The limitations are discussed in Section 5.4.

   Guidelines:

   - The answer NA means that the paper has no limitation while the answer No means that the paper has limitations, but those are not discussed in the paper.
   - The authors are encouraged to create a separate "Limitations" section in their paper.
   - The paper should point out any strong assumptions and how robust the results are to violations of these assumptions (e.g., independence assumptions, noiseless settings, model well-specification, asymptotic approximations only holding locally). The authors should reflect on how these assumptions might be violated in practice and what the implications would be.
   - The authors should reflect on the scope of the claims made, e.g., if the approach was only tested on a few datasets or with a few runs. In general, empirical results often depend on implicit assumptions, which should be articulated.
   - The authors should reflect on the factors that influence the performance of the approach. For example, a facial recognition algorithm may perform poorly when image resolution is low or images are taken in low lighting. Or a speech-to-text system might not be used reliably to provide closed captions for online lectures because it fails to handle technical jargon.
   - The authors should discuss the computational efficiency of the proposed algorithms and how they scale with dataset size.
   - If applicable, the authors should discuss possible limitations of their approach to address problems of privacy and fairness.
   - While the authors might fear that complete honesty about limitations might be used by reviewers as grounds for rejection, a worse outcome might be that reviewers discover limitations that aren't acknowledged in the paper. The authors should use their best judgment and recognize that individual actions in favor of transparency play an important role in developing norms that preserve the integrity of the community. Reviewers will be specifically instructed to not penalize honesty concerning limitations.

3. **Theory assumptions and proofs**

Question: For each theoretical result, does the paper provide the full set of assumptions and a complete (and correct) proof?

Answer: [Yes]

Justification: The proofs for the theoretical results are found in Appendix A.1.

Guidelines:

- The answer NA means that the paper does not include theoretical results.
- All the theorems, formulas, and proofs in the paper should be numbered and cross-referenced.
- All assumptions should be clearly stated or referenced in the statement of any theorems.
- The proofs can either appear in the main paper or the supplemental material, but if they appear in the supplemental material, the authors are encouraged to provide a short proof sketch to provide intuition.
- Inversely, any informal proof provided in the core of the paper should be complemented by formal proofs provided in appendix or supplemental material.
- Theorems and Lemmas that the proof relies upon should be properly referenced.

4. **Experimental result reproducibility**

Question: Does the paper fully disclose all the information needed to reproduce the main experimental results of the paper to the extent that it affects the main claims and/or conclusions of the paper (regardless of whether the code and data are provided or not)?

Answer: [Yes]

Justification: The algorithm and estimator are described in full in Section 4, and the experiments, with all relevant parameters and equations, as well as algorithm hyperparameters, are described in Section 5.

Guidelines:

- The answer NA means that the paper does not include experiments.
- If the paper includes experiments, a No answer to this question will not be perceived well by the reviewers: Making the paper reproducible is important, regardless of whether the code and data are provided or not.
- If the contribution is a dataset and/or model, the authors should describe the steps taken to make their results reproducible or verifiable.
- Depending on the contribution, reproducibility can be accomplished in various ways. For example, if the contribution is a novel architecture, describing the architecture fully might suffice, or if the contribution is a specific model and empirical evaluation, it may be necessary to either make it possible for others to replicate the model with the same dataset, or provide access to the model. In general. releasing code and data is often one good way to accomplish this, but reproducibility can also be provided via detailed instructions for how to replicate the results, access to a hosted model (e.g., in the case of a large language model), releasing of a model checkpoint, or other means that are appropriate to the research performed.
- While NeurIPS does not require releasing code, the conference does require all submissions to provide some reasonable avenue for reproducibility, which may depend on the nature of the contribution. For example
  (a) If the contribution is primarily a new algorithm, the paper should make it clear how to reproduce that algorithm.
  (b) If the contribution is primarily a new model architecture, the paper should describe the architecture clearly and fully.
  (c) If the contribution is a new model (e.g., a large language model), then there should either be a way to access this model for reproducing the results or a way to reproduce the model (e.g., with an open-source dataset or instructions for how to construct the dataset).
  (d) We recognize that reproducibility may be tricky in some cases, in which case authors are welcome to describe the particular way they provide for reproducibility. In the case of closed-source models, it may be that access to the model is limited in some way (e.g., to registered users), but it should be possible for other researchers to have some path to reproducing or verifying the results.

5. **Open access to data and code**

   Question: Does the paper provide open access to the data and code, with sufficient instructions to faithfully reproduce the main experimental results, as described in supplemental material?

   Answer: [No]

   Justification: We do not include external code or data in this submission but all data are synthetic and fully specified in the paper, and our algorithmic procedures are described in enough detail to reproduce the results.

   Guidelines:

   - The answer NA means that paper does not include experiments requiring code.
   - Please see the NeurIPS code and data submission guidelines (https://nips.cc/public/guides/CodeSubmissionPolicy) for more details.
   - While we encourage the release of code and data, we understand that this might not be possible, so No is an acceptable answer. Papers cannot be rejected simply for not including code, unless this is central to the contribution (e.g., for a new open-source benchmark).
   - The instructions should contain the exact command and environment needed to run to reproduce the results. See the NeurIPS code and data submission guidelines (https://nips.cc/public/guides/CodeSubmissionPolicy) for more details.
   - The authors should provide instructions on data access and preparation, including how to access the raw data, preprocessed data, intermediate data, and generated data, etc.
   - The authors should provide scripts to reproduce all experimental results for the new proposed method and baselines. If only a subset of experiments are reproducible, they should state which ones are omitted from the script and why.
   - At submission time, to preserve anonymity, the authors should release anonymized versions (if applicable).
   - Providing as much information as possible in supplemental material (appended to the paper) is recommended, but including URLs to data and code is permitted.

6. **Experimental setting/details**

   Question: Does the paper specify all the training and test details (e.g., data splits, hyperparameters, how they were chosen, type of optimizer, etc.) necessary to understand the results?

   Answer: [Yes]

   Justification: All hyperparameters chosen for experiments are described in Section 5.

   Guidelines:

   - The answer NA means that the paper does not include experiments.
   - The experimental setting should be presented in the core of the paper to a level of detail that is necessary to appreciate the results and make sense of them.
   - The full details can be provided either with the code, in appendix, or as supplemental material.

7. **Experiment statistical significance**

   Question: Does the paper report error bars suitably and correctly defined or other appropriate information about the statistical significance of the experiments?

   Answer: [Yes]

   Justification: The primary experimental figures (e.g., Figures 4, 7 and 12) consistently report error bars. These are explicitly defined in the figure captions as two Monte Carlo standard errors.

   Guidelines:

   - The answer NA means that the paper does not include experiments.
   - The authors should answer "Yes" if the results are accompanied by error bars, confidence intervals, or statistical significance tests, at least for the experiments that support the main claims of the paper.

- The factors of variability that the error bars are capturing should be clearly stated (for example, train/test split, initialization, random drawing of some parameter, or overall run with given experimental conditions).
- The method for calculating the error bars should be explained (closed form formula, call to a library function, bootstrap, etc.)
- The assumptions made should be given (e.g., Normally distributed errors).
- It should be clear whether the error bar is the standard deviation or the standard error of the mean.
- It is OK to report 1-sigma error bars, but one should state it. The authors should preferably report a 2-sigma error bar than state that they have a 96% CI, if the hypothesis of Normality of errors is not verified.
- For asymmetric distributions, the authors should be careful not to show in tables or figures symmetric error bars that would yield results that are out of range (e.g. negative error rates).
- If error bars are reported in tables or plots, The authors should explain in the text how they were calculated and reference the corresponding figures or tables in the text.

8. **Experiments compute resources**

   Question: For each experiment, does the paper provide sufficient information on the computer resources (type of compute workers, memory, time of execution) needed to reproduce the experiments?

   Answer: [Yes]

   Justification: Yes, the results of each experiment include required likelihood evaluations, which provide a hardware-agnostic metric for evaluating compute cost.

   Guidelines:

   - The answer NA means that the paper does not include experiments.
   - The paper should indicate the type of compute workers CPU or GPU, internal cluster, or cloud provider, including relevant memory and storage.
   - The paper should provide the amount of compute required for each of the individual experimental runs as well as estimate the total compute.
   - The paper should disclose whether the full research project required more compute than the experiments reported in the paper (e.g., preliminary or failed experiments that didn't make it into the paper).

9. **Code of ethics**

   Question: Does the research conducted in the paper conform, in every respect, with the NeurIPS Code of Ethics `https://neurips.cc/public/EthicsGuidelines`?

   Answer: [Yes]

   Justification: We confirm that this research was conducted according to the NeurIPS Code of Ethics.

   Guidelines:

   - The answer NA means that the authors have not reviewed the NeurIPS Code of Ethics.
   - If the authors answer No, they should explain the special circumstances that require a deviation from the Code of Ethics.
   - The authors should make sure to preserve anonymity (e.g., if there is a special consideration due to laws or regulations in their jurisdiction).

10. **Broader impacts**

    Question: Does the paper discuss both potential positive societal impacts and negative societal impacts of the work performed?

    Answer: [NA]

    Justification: This work is purely foundational research, and we do not identify any specific positive or negative social impacts beyond those of general advances in machine learning methodology.

Guidelines:

- The answer NA means that there is no societal impact of the work performed.
- If the authors answer NA or No, they should explain why their work has no societal impact or why the paper does not address societal impact.
- Examples of negative societal impacts include potential malicious or unintended uses (e.g., disinformation, generating fake profiles, surveillance), fairness considerations (e.g., deployment of technologies that could make decisions that unfairly impact specific groups), privacy considerations, and security considerations.
- The conference expects that many papers will be foundational research and not tied to particular applications, let alone deployments. However, if there is a direct path to any negative applications, the authors should point it out. For example, it is legitimate to point out that an improvement in the quality of generative models could be used to generate deepfakes for disinformation. On the other hand, it is not needed to point out that a generic algorithm for optimizing neural networks could enable people to train models that generate Deepfakes faster.
- The authors should consider possible harms that could arise when the technology is being used as intended and functioning correctly, harms that could arise when the technology is being used as intended but gives incorrect results, and harms following from (intentional or unintentional) misuse of the technology.
- If there are negative societal impacts, the authors could also discuss possible mitigation strategies (e.g., gated release of models, providing defenses in addition to attacks, mechanisms for monitoring misuse, mechanisms to monitor how a system learns from feedback over time, improving the efficiency and accessibility of ML).

11. **Safeguards**

    Question: Does the paper describe safeguards that have been put in place for responsible release of data or models that have a high risk for misuse (e.g., pretrained language models, image generators, or scraped datasets)?

    Answer: [NA]

    Justification: The paper poses no such risks.

    Guidelines:

    - The answer NA means that the paper poses no such risks.
    - Released models that have a high risk for misuse or dual-use should be released with necessary safeguards to allow for controlled use of the model, for example by requiring that users adhere to usage guidelines or restrictions to access the model or implementing safety filters.
    - Datasets that have been scraped from the Internet could pose safety risks. The authors should describe how they avoided releasing unsafe images.
    - We recognize that providing effective safeguards is challenging, and many papers do not require this, but we encourage authors to take this into account and make a best faith effort.

12. **Licenses for existing assets**

    Question: Are the creators or original owners of assets (e.g., code, data, models), used in the paper, properly credited and are the license and terms of use explicitly mentioned and properly respected?

    Answer: [NA]

    Justification: The paper does not use existing assets.

    Guidelines:

    - The answer NA means that the paper does not use existing assets.
    - The authors should cite the original paper that produced the code package or dataset.
    - The authors should state which version of the asset is used and, if possible, include a URL.
    - The name of the license (e.g., CC-BY 4.0) should be included for each asset.

- For scraped data from a particular source (e.g., website), the copyright and terms of service of that source should be provided.
- If assets are released, the license, copyright information, and terms of use in the package should be provided. For popular datasets, paperswithcode.com/datasets has curated licenses for some datasets. Their licensing guide can help determine the license of a dataset.
- For existing datasets that are re-packaged, both the original license and the license of the derived asset (if it has changed) should be provided.
- If this information is not available online, the authors are encouraged to reach out to the asset's creators.

13. **New assets**

    Question: Are new assets introduced in the paper well documented and is the documentation provided alongside the assets?

    Answer: [NA]

    Justification: This paper does not release new assets.

    Guidelines:

    - The answer NA means that the paper does not release new assets.
    - Researchers should communicate the details of the dataset/code/model as part of their submissions via structured templates. This includes details about training, license, limitations, etc.
    - The paper should discuss whether and how consent was obtained from people whose asset is used.
    - At submission time, remember to anonymize your assets (if applicable). You can either create an anonymized URL or include an anonymized zip file.

14. **Crowdsourcing and research with human subjects**

    Question: For crowdsourcing experiments and research with human subjects, does the paper include the full text of instructions given to participants and screenshots, if applicable, as well as details about compensation (if any)?

    Answer: [NA]

    Justification: This paper does not involve crowdsourcing or research with human subjects.

    Guidelines:

    - The answer NA means that the paper does not involve crowdsourcing nor research with human subjects.
    - Including this information in the supplemental material is fine, but if the main contribution of the paper involves human subjects, then as much detail as possible should be included in the main paper.
    - According to the NeurIPS Code of Ethics, workers involved in data collection, curation, or other labor should be paid at least the minimum wage in the country of the data collector.

15. **Institutional review board (IRB) approvals or equivalent for research with human subjects**

    Question: Does the paper describe potential risks incurred by study participants, whether such risks were disclosed to the subjects, and whether Institutional Review Board (IRB) approvals (or an equivalent approval/review based on the requirements of your country or institution) were obtained?

    Answer: [NA]

    Justification: This paper does not involve crowdsourcing or research with human subjects.

    Guidelines:

    - The answer NA means that the paper does not involve crowdsourcing nor research with human subjects.

- Depending on the country in which research is conducted, IRB approval (or equivalent) may be required for any human subjects research. If you obtained IRB approval, you should clearly state this in the paper.
- We recognize that the procedures for this may vary significantly between institutions and locations, and we expect authors to adhere to the NeurIPS Code of Ethics and the guidelines for their institution.
- For initial submissions, do not include any information that would break anonymity (if applicable), such as the institution conducting the review.

16. **Declaration of LLM usage**

    Question: Does the paper describe the usage of LLMs if it is an important, original, or non-standard component of the core methods in this research? Note that if the LLM is used only for writing, editing, or formatting purposes and does not impact the core methodology, scientific rigorousness, or originality of the research, declaration is not required.

    Answer: [NA] .

    Justification: This research does not involve or use LLMs in any way.

    Guidelines:

    - The answer NA means that the core method development in this research does not involve LLMs as any important, original, or non-standard components.
    - Please refer to our LLM policy (https://neurips.cc/Conferences/2025/LLM) for what should or should not be described.